Available online at www.sciencedirect.com
ScienceDirect
Journal of Power Sources 158 (2006) 1084–1090
JOURNAL OF POWER SOURCES
www.elsevier.com/locate/jpowsour

Development of additives in negative active-material to suppress sulfation during high-rate partial-state-of-charge operation of lead–acid batteries

Ken Sawai [a,*], Takayuki Funato [a], Masashi Watanabe [a], Hidetoshi Wada [a], Kenji Nakamura [a], Masaaki Shiomi [b], Shigeharu Osumi [a]

[a] *GS Yuasa Manufacturing Ltd., Kyoto, Japan*
[b] *GS Yuasa Corporation Ltd., Kyoto, Japan*

Received 1 August 2005; accepted 27 January 2006
Available online 24 March 2006

Abstract

Additives in the negative active-material of lead–acid batteries were examined to determine whether they could prevent progressive accumulation of lead sulfate ($PbSO_4$) in negative plates during high-rate partial-state-of-charge (HRPSoC) operation. This phenomenon is caused by progressive growth of $PbSO_4$ particles and a lack of conductive paths near these $PbSO_4$ particles.

Barium sulfate ($BaSO_4$) particles in various sizes and synthetic lignin were added to the negative active-material to control $PbSO_4$ particle size during HRPSoC cycle-life. Some types of carbon fibres were also added to form conductive paths around the $PbSO_4$ particles. Synthetic lignin was found to be the most effective additive for improving battery life in HRPSoC cycle-life tests, whereas the other factors such as $BaSO_4$ size or carbon fibre extended less influence. The growth rate of $PbSO_4$ particles per cycle was much lower in a cell with synthetic lignin than in a cell with natural lignin.

Keywords: Lead–acid battery; High-rate partial-state-of-charge; Negative active-material; Barium sulfate; Synthetic lignin; Carbon

1. Introduction

Lead–acid batteries for high-power duty in systems such as 42-V automobile powernets are operated under high-rate partial-state-of-charge (HRPSoC) conditions [1]. The life-limiting mechanism of lead–acid batteries in this application involves progressive accumulation of lead sulfate ($PbSO_4$) in negative plates [2]. This failure mode is commonly called 'sulfation'.

It has been reported [3–6] that addition of highly conductive carbon to negative active-material is effective in arresting sulfation. Discharged negative active-material can be recharged more easily with highly conductive carbon, but this carbon cannot prevent the progressive growth of the $PbSO_4$ particles. Therefore, the effect of carbon on the rechargeability of negative plates is attributed to a volumetric connection between the carbon particles, which form conductive paths between $PbSO_4$ particles in the negative active-material [6]. Other materials are being tested to prevent progressive growth of $PbSO_4$ particles and for better conductive paths.

Barium sulfate ($BaSO_4$) is considered to work as a nucleus for $PbSO_4$ [7]. Therefore, increasing amounts of barium sulfate, or barium sulfate particles with a small size, have been added to increase the number of $PbSO_4$ nuclei. The relationship between the amounts of barium sulfate, or the size of barium sulfate particles, and $PbSO_4$ particle diameter after discharge have been investigated.

Natural lignin is generally added to the negative active-material. The molecular construction of a natural lignin is shown in Fig. 1. On the other hand, a high-performance synthetic lignin has been developed; the molecular structure is shown in Fig. 2. The efficacy of this synthetic lignin has been evaluated under an EV schedule (with deep discharge and full recharge). The results for batteries with these two types of lignin are given in Fig. 3. The data show that the cycle-life performance of the battery with synthetic lignin is superior to that with natural lignin [8]. Therefore, this study reports an evaluation of the syn-

* Corresponding author at: Technical Center, GS Yuasa Manufacturing Ltd., Nishinosho, Kisshoin, Minami-ku, Kyoto 601-8520, Japan. Tel.: +81 75 316 3626; fax: +81 75 316 3798.
E-mail address: ken.sawai@ip.gs-yuasa.com (K. Sawai).

0378-7753/$ – see front matter © 2006 Elsevier B.V. All rights reserved.
doi:10.1016/j.jpowsour.2006.01.096

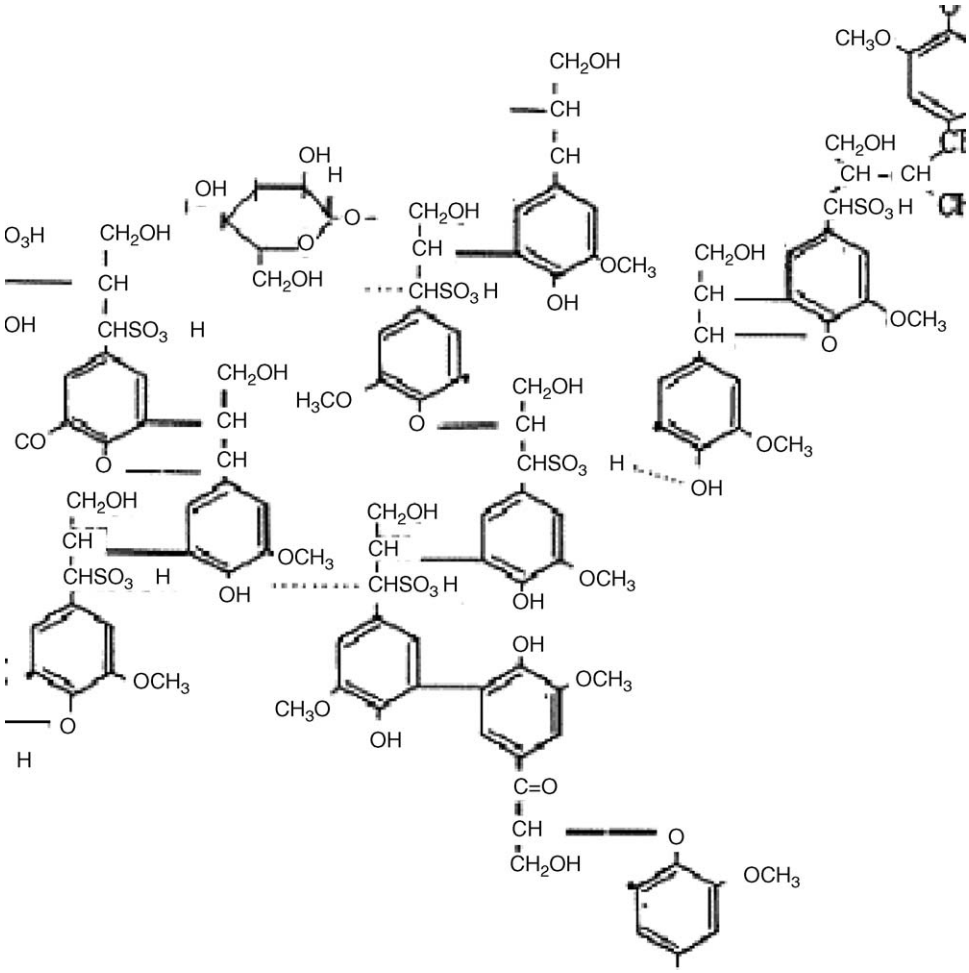

Fig. 1. Schematic formula of natural lignin structure.

thetic lignin as a means for suppressing sulfation under HRPSoC operation.

2. Experimental

Test cells (2 V, 16 Ah) were assembled with various types of additive in the negative active-material. The cells were subjected to an HRPSoC cycle-life test. The additives were $BaSO_4$ particles of different diameter, new synthetic lignin, and carbon fibres. After the HRPSoC cycle-life test, cells were disassembled and the size of the $PbSO_4$ particles in the negative active-material was measured by the BET surface-area technique.

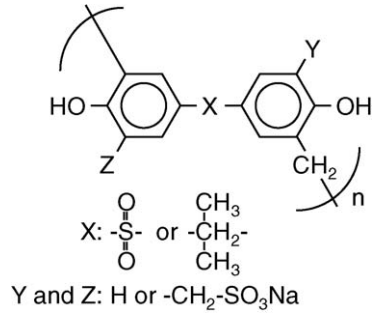

Fig. 2. Schematic formula of synthetic lignin.

2.1. Preparation of additives

2.1.1. Barium sulfate

A scanning electron micrograph of standard commercial barium sulfate is shown in Fig. 4(a). It has a mean particle size of 2.4 μm by catalog value. In fact, the particles agglomerated so that the mean diameter of the particles, as measured and counted

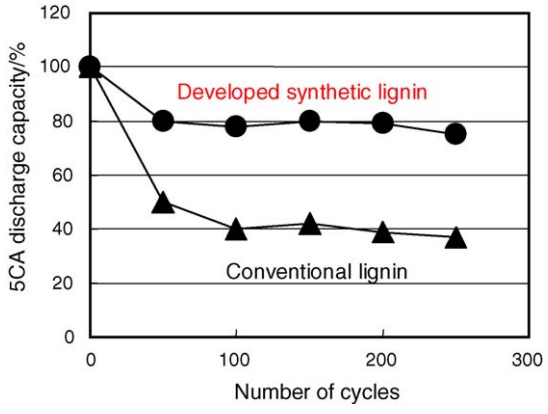

Fig. 3. Cycle-life results of cells with (▲) natural lignin and (●) synthetic lignin. Cycle conditions: discharge by 0.33 CA for 2.4 h (80% DoD); charged by 0.5 CA for 1.3 h and by 0.1 CA for 2.3 h (110% of discharge) at 50 °C.

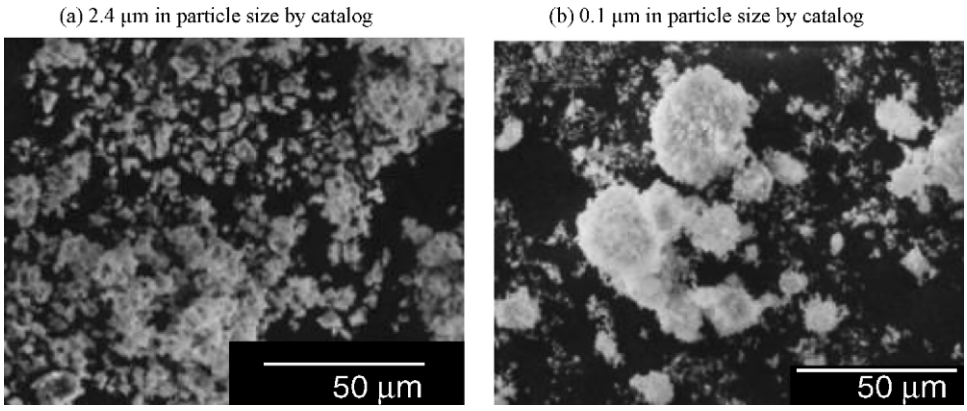

Fig. 4. Scanning electron micrographs of commercial barium sulfate. Mean diameter size: (a) 2.4 μm; (b) 0.1 μm; by catalog.

from the micrograph, is 7.4 μm. A micrograph of commercial barium sulfate with 0.1 μm mean particle size by catalog value is given in Fig. 4(b). Again, it is found that the small barium sulfate particles agglomerate into larger particles; mean diameter is 23.0 μm. In order to add small particles of barium sulfate to negative active-material, agglomeration must be prevented.

Commercial barium sulfate is made by reacting barium sulfide and sodium sulfate in aqueous solution. With this method, small barium sulfate particles are formed. They are then dried to a powder state and it is during this step that agglomeration takes place. Therefore, by omitting the drying stage, it is possible to add barium sulfate of smaller particle size to negative active-material.

The particle diameters of powder and aqueous suspension samples of barium sulfate were measured. Details of the samples are given in Table 1. Sample A is a commercial barium sulfate and its mean particle diameter is 0.1 μm by catalog. Sample B is the aqueous suspension that was dried to prepare sample A. Samples C–E have been specially made from barium hydroxide solution and sulfuric acid. Barium hydroxide is used in this process instead of barium sulfide, so as not to leave sulfide ions in the suspension after reaction. In addition, in the production process, concentration of sulfuric acid and reaction temperature are all controlled.

The float-specific gravity meter method (FSGM method) [9] was selected to measure the particle-size distribution. A schematic diagram of FSGM method is given in Fig. 5. The procedure was as follows:

(i) Barium sulfate (30 g) was added to 1000 ml of water, and stirred well.

Table 1
Samples of barium sulfate added to negative active-material

Barium sulfate	Production type	Reaction condition	
		Reaction temperature (°C)	Relative density of H_2SO_4 at 20 °C
Powder A	Commercial	–	–
Suspension B	Commercial	–	–
Suspension C	Specially made	10	1.10
Suspension D	Specially made	10	1.40
Suspension E	Specially made	60	1.40

(ii) The suspension was put into a 1000-ml measuring cylinder. The latter was covered and turned upside down slowly two or three times for agitation. The suspension was then allowed to settle.
(iii) Float-specific gravity meter was put into the suspension and scale L_1 was recorded.
(iv) Scale L_1 and the measured time t were recorded repeatedly while the suspension stayed calm.

The distribution of the diameters of the barium sulfate particles in the suspension is calculated as follows:

$$D = \sqrt{\frac{30 \times \mu \times H}{980 \times (\rho_0 - \rho_1) \times t}} \quad (1)$$

$$H = L_1 + \frac{1}{2}L_2 \quad (2)$$

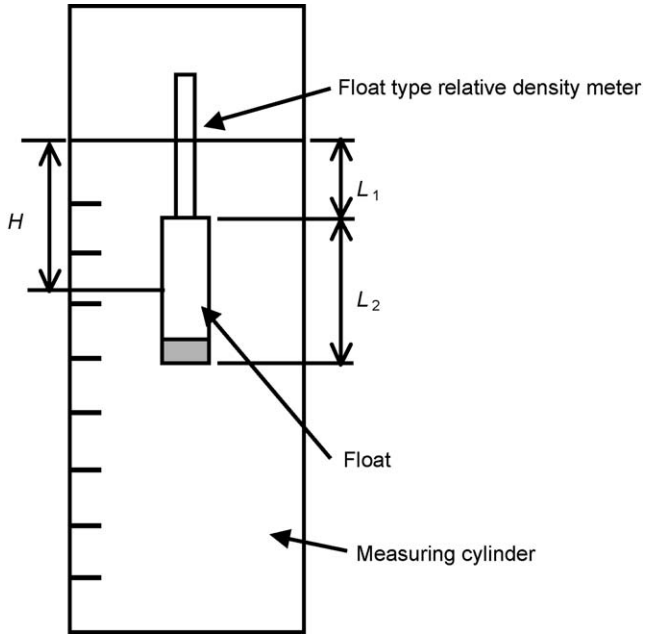

Fig. 5. Schematic of effective height H in float-specific gravity meter method (FSGM method). Parameters H, L_1, and L_2 are defined in text.

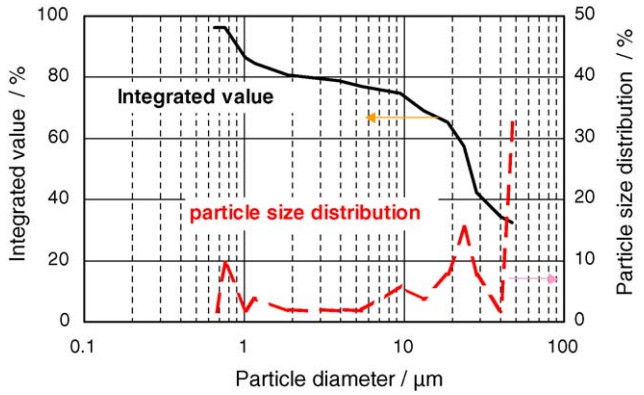

Fig. 6. Particle-size distribution of barium sulfate powder A by FSGM method.

where D is the diameter of barium sulfate (mm), μ the viscosity coefficient (1 g cm^{-1} s^{-1}), H the effective height (cm), ρ_0 the density of barium sulfate (4.5 g cm^{-3}), ρ_1 the density of suspension, measured value, t the measured time, L_1 the distance from top of float to suspension level recorded on scale (cm) and L_2 is the float length of specific gravity meter (cm).

Thus, the symbol D refers to the maximum particle diameter at point H in a suspension of specific gravity ρ_1 at time t.

The particle-size distribution of sample A measured by the FSGM method is presented in Fig. 6. There are two peaks at 0.8 and 25 μm, and the mean diameter (at which the integrated value of the particle mass was 50%) was 26.1 μm. By comparison, the mean particle diameter calculated from scanning electron micrographs was 23.0 μm. The results of the FSGM method were therefore in a good agreement with those calculated from micrographs.

The mean diameter of sample B was 0.5 μm by the FSGM method, and almost all the particles were less than 1 μm. Thus, the particle size of barium sulfate without drying was about 1/50th that of dried barium sulfate.

The relationship between mean particle diameter and reaction conditions is demonstrated in Fig. 7. The particle size of barium sulfate becomes smaller with increasing concentration of sulfuric acid and with decreasing reaction temperature.

2.1.2. Other additives

Natural lignin A is generally used for lead–acid batteries. The molecular structures of an example of natural lignin and the synthetic lignin B are given in Figs. 1 and 2, respectively. The synthetic lignin B is a mixed polymer of unit structures with functional groups X–Z.

Table 2
Samples of carbon added to negative active-material

Carbon	Fibre length (mm)	Diameter of fibre (μm)	Diameter of particle (μm)	Specific electric resistance (mΩ)
Powder A	–	–	35	0.015
Fibre B	0.13	13	–	0.010
Fibre C	1.5	13	–	0.010

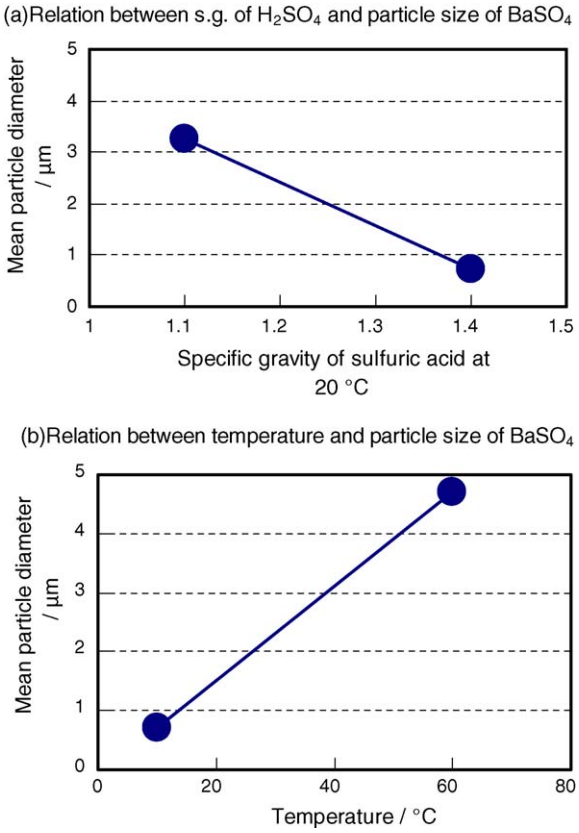

Fig. 7. Effects of (a) concentration of sulfuric acid and (b) reaction temperature on mean particle diameter of barium sulfate.

The characteristics of the carbon fibres are shown in Table 2. Samples B and C are cured carbon fibres. Scanning electron micrographs of carbon fibres and carbon in unformed negative plates are shown in Fig. 8.

2.2. Cycle-life testing

2.2.1. Test cell

Valve-regulated cells (2 V, 16 Ah at 10-h rate) were assembled with three positive plates and two negative plates and absorptive glass–mat separators. The additives in the negative active-material were 0.3 wt.% barium sulfate powder A, natural lignin A, and carbon powder A. The electrolyte was 4.88 M (specific gravity 1.28 at 20 °C) H_2SO_4.

2.2.2. Test regime

The initial discharge capacity of the cells was first determined. The cells were discharged at the 1CA rate at 25 °C. Then, the cells were tested under constant-current charge–discharge HRPSoC conditions at 25 °C. Cycle regime was as follows:

Pre-discharge	1 CA × 4 min (10% DoD)
Discharge	1 CA × 12 min (40% DoD)
Charge	1 CA × 12 min (10% DoD)

After every 300 cycles, the 1 CA discharge capacity was checked at 25 °C.

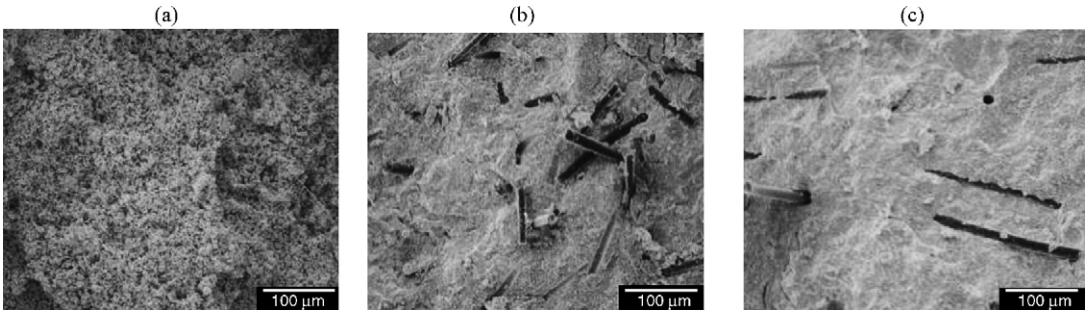

Fig. 8. Scanning electron micrographs of carbon or carbon fibre in unformed negative active-material with (a) powder A, (b) fibre B, and (c) fibre C.

2.2.3. Measurement of size of lead sulfate particles

The test cells were disassembled after discharge and the negative plates were washed and dried. The accumulation of $PbSO_4$ in the negative active-material was determined and the lead metal in negative active-material was etched. The BET-specific surface-area of the etched sample was measured to calculate the mean diameter of the $PbSO_4$ particles. Although the size can be measured by SEM the micrographs have a very small range of vision and many images have to be taken to determine the mean diameter of $PbSO_4$ particles in the whole negative active-material. Therefore, the size of the particles was calculated from measurements of BET-specific surface-area.

If the $PbSO_4$ particle is assumed to be a sphere (radius = r, density = 6.23 g cm^{-3}), the diameter ($R = 2r$) can be calculated from the BET-specific surface-area S (m^2 g^{-1}) by the following formula:

$$S = \text{surface area of a sphere/mass of a sphere} = \frac{4\pi r^2}{(4/3)\pi r^3 \times 6.23 \times 10^6} = \frac{0.4815 \times 10^{-6}}{r} \quad (3)$$

$$R = 2r = 2 \times 0.4815 \times 10^{-6}/S\,[\text{m}] = 0.9630/S\,[\mu\text{m}] \quad (4)$$

3. Results and discussion

3.1. Barium sulfate

First, the particle diameter of $PbSO_4$ after initial discharge was measured.

The relationship between the amount of barium sulfate and the mean particle diameter of $PbSO_4$ calculated from BET-specific surface-area after first discharge is given in Fig. 9. The particle diameter of $PbSO_4$ became smaller when more barium sulfate was added. The influence of the amount of barium sulfate above 0.3 wt.% on $PbSO_4$ size was, however, quite small.

The relationship between the size of barium sulfate particles and the mean particle diameter of $PbSO_4$ as calculated from the BET-specific surface-area, is presented in Fig. 10. The data show that the smaller the barium sulfate, the smaller the $PbSO_4$ diameter after discharge. The particle diameter of the particles is less than that of particles obtained when using 3 mass% of larger barium sulfate. In summary, it is possible to reduce the size of $PbSO_4$ particles in negative active-material after discharge by increasing the amount of barium sulfate and by adding smaller barium sulfate particles at the initial stage of battery life.

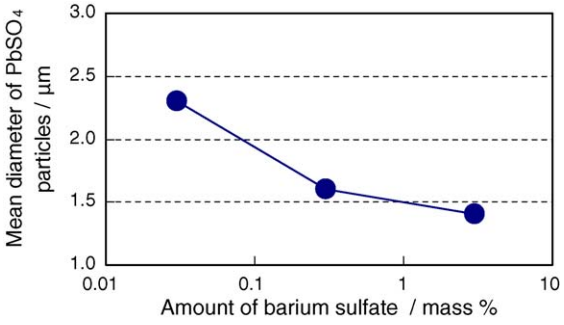

Fig. 9. Relationship between amount of barium sulfate and mean particle diameter of $PbSO_4$ after etching process.

The duration of discharge after every 300 cycles of the HRP-SoC test is shown in Fig. 11. The cycle-life performance is not improved by controlling the $PbSO_4$ size at initial discharge.

After the constant-current cycle-life test, the test cells were disassembled. The accumulation and diameter of the $PbSO_4$ particles in the negative active-material were both determined. The results are given in Table 3.

Scanning electron micrographs of each sample after the etching process are presented in Fig. 12. The investigations show that the $PbSO_4$ particle diameter at the initial stage of cycle-life does not affect the particle size after the cycle-life test. From these results, the initial $PbSO_4$ particle diameter, as controlled by barium sulfate, does not influence HRPSoC performance.

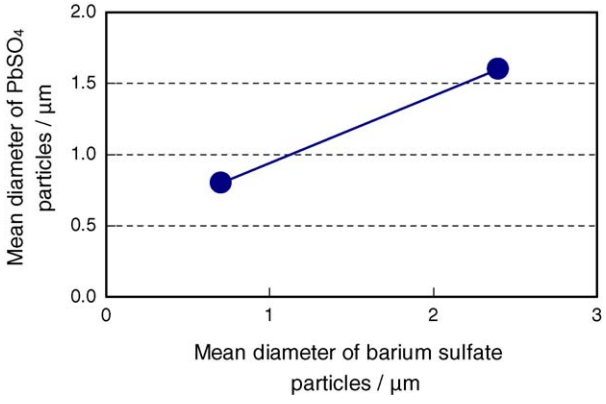

Fig. 10. Relationship between barium sulfate particle diameter and mean particle diameter of $PbSO_4$ after etching process.

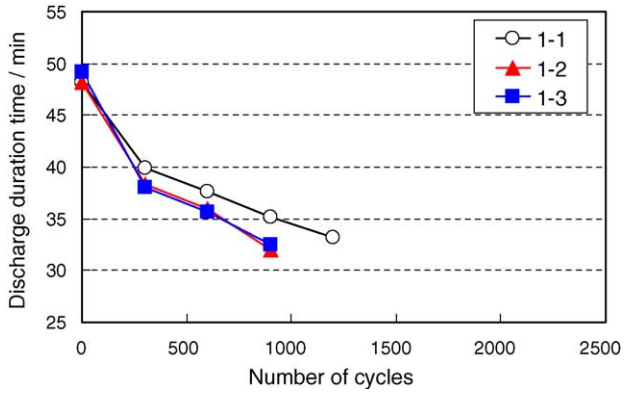

Fig. 11. Change in discharge time during constant-current HRPSoC cycling of cells with (◯) $BaSO_4$ powder A; (▲) $BaSO_4$ suspension B; (■) $BaSO_4$ suspension D.

Table 3
Amount and particle diameter of $PbSO_4$ in negative active-material after constant-current HRPSoC cycle-life test

Cell No.	Amount of $PbSO_4$ (mass.%)	$PbSO_4$ particle diameter from BET* (μm)
1-1	31	3.0
1-2	29	3.1
1-3	28	3.0

* Excluding carbon by calculation.

3.2. Synthetic lignin

The discharge time after every 300 cycles of the HRPSoC life test for cells with natural lignin A and synthetic lignin B is given in Fig. 13. The cells with the latter additive lasted much longer than that with natural lignin A. The cells were disassembled. The amount of $PbSO_4$ in the negative active-material was measured and the particle diameter of $PbSO_4$ in the negative active-material was calculated from measurements of BET-specific surface-area. The amount of accumulated $PbSO_4$ and the $PbSO_4$ particle diameter are listed in Table 4. The amount of $PbSO_4$ with synthetic lignin B in cells Nos. 2-2 and 2-3 did not increase, even after the longer cycle-life sustained by these cells. In addition, there was little increase in $PbSO_4$ particle diameter.

Scanning electron micrographs of the negative active-material of the cells after the cycle-life test, and before the etching process are presented in Fig. 14. The $PbSO_4$ particles

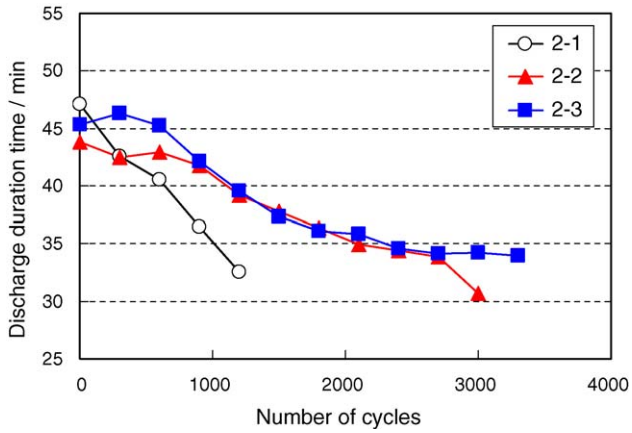

Fig. 13. Change in discharge time during constant-current HRPSoC cycle-life test of cells with (◯) $BaSO_4$ powder A and natural lignin A; (▲) $BaSO_4$ powder A and synthetic lignin B; (■) $BaSO_4$ suspension D and synthetic lignin B.

Table 4
Amount and particle diameter of $PbSO_4$ in negative active-material after constant-current HRPSoC cycle-life test

Cell No.	Amount of $PbSO_4$ (mass.%)	$PbSO_4$ particle diameter from BET* (μm)
2-1	29	3.1
2-2	26	3.4
2-3	27	3.7

* Excluding carbon by calculation.

in cells with synthetic lignin B were more uniform in size than those in the cell with natural lignin A, even after much longer life. Thus synthetic lignin B prevents progressive growth of $PbSO_4$ particles during HRPSoC duty.

Synthetic lignin B markedly improved HRPSoC performance. The accumulation of $PbSO_4$ and the particle diameter were almost the same when natural lignin A was used, irrespective of the respective cycle lives.

Therefore, the rate of growth of $PbSO_4$ particles per cycle was much lower in cells with synthetic lignin B.

3.3. Carbon fibres

The discharge time after every 300 HRPSoC cycles for cells with fibre A and powder A is given in Fig. 15. Cell 3-1 with

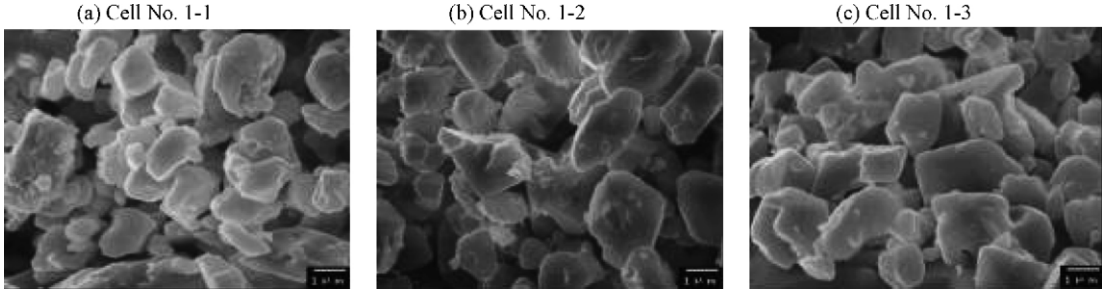

Fig. 12. Scanning electron micrographs of negative active-material of cells with (a) $BaSO_4$ powder A; (b) $BaSO_4$ suspension B; (c) $BaSO_4$ suspension D; after constant-current HRPSoC cycle-life test, after etching process.

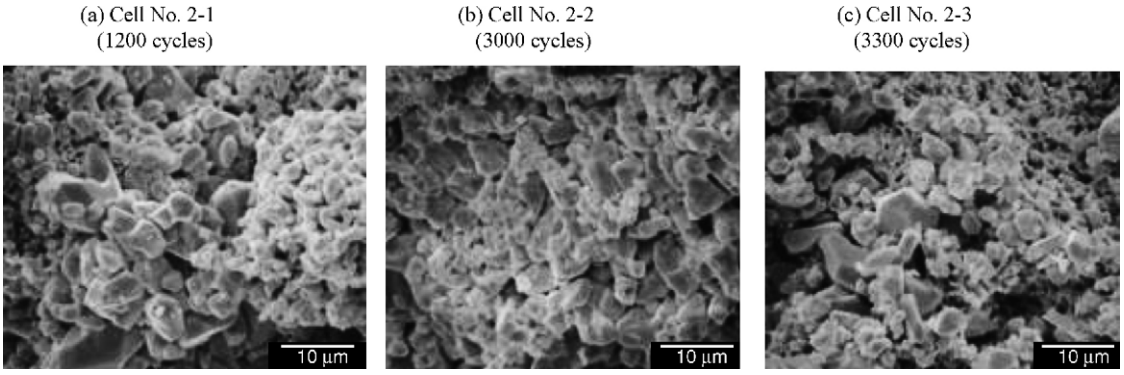

Fig. 14. Scanning electron micrographs of negative active-material of cells with (a) $BaSO_4$ powder A and natural lignin A; (b) $BaSO_4$ powder A and synthetic lignin B; (c) $BaSO_4$ suspension D and synthetic lignin B; before etching process.

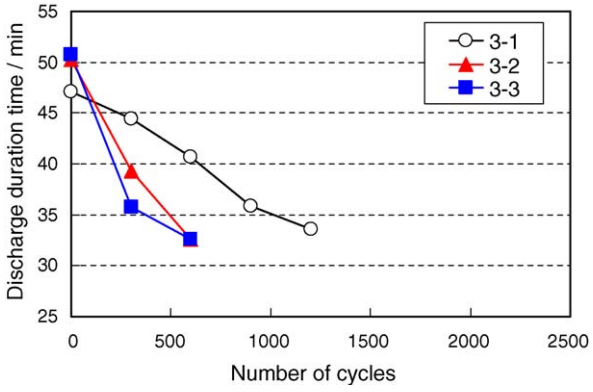

Fig. 15. Change in discharge time during constant-current HRPSoC cycle-life test of cells with: (◯) carbon powder A; (▲) carbon fibre B; (■) carbon fibre C.

Table 5
Amount and particle diameter of $PbSO_4$ in negative active-material after constant-current HRPSoC cycle-life test

Cell No.	Amount of $PbSO_4$ (mass.%)	$PbSO_4$ particle diameter from BET* (μm)
3-1	31	2.8
3-2	35	2.7
3-3	32	2.7

* Excluding carbon by calculation.

carbon powder A delivered a larger capacity than those of the cells with fibre B or C.

The cells were disassembled and analyzed. It was found that amount of accumulated $PbSO_4$ and its particle diameter were almost the same when carbon powder or carbon fibre was added (see Table 5).

Carbon fibre A did not improve the capacity during HRPSoC cycling. This is because the fibres were not as dispersed as uniformly as carbon powder in the negative active-material (see Fig. 8). Therefore, it is concluded that the carbon fibres are unable to form sufficient conductive paths in $PbSO_4$, and thereby cannot improve the rechargeability of negative active-material.

4. Conclusions

Synthetic lignin was very effective in improving the HRPSoC cycle-life performance of lead–acid batteries.

The particle diameter of $PbSO_4$ developed in the presence of synthetic lignin B was almost the same as that of $PbSO_4$ formed with natural lignin A, despite the longer cycle-life of the former cells. Hence, synthetic lignin B arrested the progressive growth of $PbSO_4$ particles in the negative active-material during the HRPPSoC duty.

It was possible to reduce the size of $PbSO_4$ particles in the negative active-material after discharge by increasing the amount of barium sulfate and by adding barium sulfate particles of small size at the initial stage of battery life. On the other hand, the size and diameter of barium sulfate, as well as selected carbon fibre, were found to exert no influence on the cycle-life performance of cells subjected to HRPSoC duty.

Acknowledgement

This work was supported by the Advanced Lead Acid Battery Consortium, a program of the International Lead Zinc Research Organization Inc.

References

[1] T. Ohmae, T. Hayashi, N. Inoue, J. Power Sources 116 (2003) 105.
[2] A. Cooper, L.T. Lam, P.T. Moseley, D.A.J. Rand, in: D.A.J. Rand, P.T. Mseley, J. Garche, C.D. Parker (Eds.), Valve-regulated Lead–Acid Batteries, Elsevier, Amsterdam, 2004, pp. 549–565.
[3] T. Funato, K. Takahashi, M. Tsubota, J. Tabuchi, M. Iwata, Y. Tagawa, GS News Tech. Rep. 52 (1993) 21.
[4] T. Koike, T. Hayashi, N. Higa, K. Nishida, M. Tsubota, GS News Tech. Rep. 54 (1995) 6.
[5] K. Nakamura, M. Shiomi, K. Takahashi, M. Tsubota, J. Power Sources 59 (1996) 153.
[6] M. Shiomi, T. Funato, K. Nakamura, K. Takahashi, M. Tsubota, J. Power Sources 59 (1997) 147.
[7] D. Berndt, Maintenance-Free Batteries, Lead–Acid, Nickel/Cadmium, Nickel/Metal Hydride Handbook of Battery Technology, 2nd ed., Research Studies Press Ltd., Taunton, Somerset, England, 1997, p. 318.
[8] M. Shiomi, Proceedings of the Battery Council International 2001, Las Vegas, USA, 2001.
[9] JIS (Japan Industrial Standard) A 1204.